Impaired production of naive T lymphocytes in human T-cell leukemia virus type I-infected individuals: its implications in the immunodeficient state. *Blood* 2001;**97**:3177–83.
21. Toulza F, Heaps A, Tanaka Y, Taylor GP, Bangham CRM. High frequency of $CD4^+Foxp3^+$ cells in HTLV-1 infection: inverse correlation with HTLV-1-specific CTL response. *Blood* 2008;**111**:5047–59.
22. Walker MR, Kasprowicz DJ, Gersuk VH, Benard A, Van Landeghen M, Buckner JH, Ziegler SF. Induction of FoxP3 and acquisition of T regulatory activity by stimulated human $CD4^+CD25-$ T cells. *J Clin Invest* 2003;**112**:1437–43.
23. Kasprzycka M, Marzec M, Liu X, Zhang Q, Wasik MA. Nucleophosmin/anaplastic lymphoma kinase (NPM/ALK) oncoprotein induces the T regulatory cell phenotype by activating STAT3. *Proc Natl Acad Sci USA* 2006;**103**:9964–9.
24. Hinz S, Pagerols-Raluy L, Oberg H-H, *et al.* Foxp3 expression in pancreatic carcinoma cells as a novel mechanism of immune evasion in cancer. *Cancer Res* 2007;**67**:8344–55.
25. Kohno T, Yamada Y, Akamatsu N, Kamihira S, Imaizumi Y, Tomonaga M, Matsuyama T. Possible origin of adult T-cell leukemia/lymphoma cells from human T lymphotropic virus type-1-infected regulatory T cells. *Cancer Sci* 2005;**96**:527–33.

Retrovirology

BioMed Central

Research

Open Access

Characteristic expression of HTLV-1 basic zipper factor (HBZ) transcripts in HTLV-1 provirus-positive cells

Tetsuya Usui[1], Katsunori Yanagihara[1], Kunihiro Tsukasaki[2], Ken Murata[1], Hiroo Hasegawa[1], Yasuaki Yamada[1] and Shimeru Kamihira*[1]

Address: [1]Department of Laboratory Medicine Nagasaki University Graduate School of Biomedical Sciences, Nagasaki City, Japan and [2]Department of Hematology, Nagasaki University Graduate School of Biomedical Sciences, Nagasaki City, Japan

Email: Tetsuya Usui - t-usui@nagasaki-u.ac.jp; Katsunori Yanagihara - k-yanagi@nagasaki-u.ac.jp; Kunihiro Tsukasaki - tsukasak@nagasaki-u.ac.jp; Ken Murata - k-murata@nagasaki-u.ac.jp; Hiroo Hasegawa - hhase@nagasaki-u.ac.jp; Yasuaki Yamada - y-yamada@nagasaki-u.ac.jp; Shimeru Kamihira* - kamihira@nagasaki-u.ac.jp

* Corresponding author

Published: 22 April 2008

Retrovirology 2008, 5:34 doi:10.1186/1742-4690-5-34

Received: 6 March 2008
Accepted: 22 April 2008

This article is available from: http://www.retrovirology.com/content/5/1/34

Abstract

Background: HTLV-1 causes adult T-cell leukemia (ATL). Although there have been many studies on the oncogenesis of the viral protein Tax, the precise oncogenic mechanism remains to be elucidated. Recently, a new viral factor, HTLV-1 basic Zip factor (HBZ), encoded from the minus strand mRNA was discovered and the current models of Tax-centered ATL cell pathogenesis are in conflict with this discovery. HBZs consisting of non-spliced and spliced isoforms (HBZ-SI) are thought to be implicated in viral replication and T-cell proliferation but there is little evidence on the HBZ expression profile on a large scale.

Results: To investigate the role of HBZ-SI in HTLV-1 provirus-positive cells, the HBZ-SI and Tax mRNA loads in samples with a mixture of infected and non-infected cells were measured and then adjusted by dividing by the HTLV-I proviral load. We show here that the HBZ-SI mRNA level is 4-fold higher than non-spliced HBZ and is expressed by almost all cells harboring HTLV-1 provirus with variable intensity. The proviral-adjusted HBZ-SI and Tax quantification revealed a characteristic imbalanced expression feature of high HBZ and low Tax expression levels in primary ATL cells or high HBZ and very high Tax levels in HTLV-1-related cell lines (cell lines) compared with a standard expression profile of low HBZ and low Tax in infected cells. Interestingly, according to the mutual Tax and HBZ expression status, HTLV-1-related cell lines were subcategorized into two groups, an ATL cell type with high HBZ and low Tax levels and another type with high Tax and either high or low HBZ, which was closely related to its cell origin.

Conclusion: This is the first comprehensive study to evaluate the mutual expression profile of HBZ and Tax in provirus-positive cells, revealing that there are quantitative and relative characteristic features among infected cells, primary ATL cells, and cell lines.

Introduction

Adult T-cell leukemia (ATL) is a unique T-cell malignancy derived from T-cells infected with a retrovirus of human T-cell leukemia virus type-1 (HTLV-1) [1-3]. ATL is clinically and hematologically characterized to develop step by step through smoldering, chronic, and acute stages after a long

latency of HTLV-1 infection, revealing that ATL is a good experimental model of multi-step carcinogenesis.

Although it is a fact that HTLV-1 reaches an oncogenic event and causes ATL, the oncogenic mechanism of HTLV-1 is not fully understood. The HTLV-1 genome, in addition to the structural and enzymatic proteins gag, pol, and env, encodes the regulatory and accessory proteins tax, rex, $p12^{I}$, $p13^{II}$, and $p30^{II}$ [4,5]. Among these viral proteins, Tax, encoded by pX in a double splicing manner, is thought to be mainly implicated in the oncogenesis of ATL via indirect and direct interactions between Tax and cellular molecules [6,7]. Indeed, there have been many studies showing that Tax is expressed abundantly in infected T-cells and HTLV-1-associated cell lines, and Tax acts as a main player indispensable for the malignant transformation of infected cells in the early stage of ATL development. However, ATL cells often contain genetic and epigenetic alterations of the 5'LTR of the HTLV-1 provirus, resulting in the loss of Tax expression [8]. On the other hand, the 3' end of the provirus encompassing the Tax gene is invariably maintained in leukemic cells from patients suggesting the possibility of minus strand transcription.

A novel viral protein, HTLV-1 basic zipper factor (HBZ), which is encoded by the minus strand RNA of the HTLV-1 genome, has been identified recently [9,10]. We and others identified and sequenced a novel splicing form of HBZ transcripts, named HBZ-splicing isoform (SI), which encodes a 206 amino acid protein and is generated by alternative splicing between part of the HBZ gene and a novel exon located in the 3' LTR of the HTLV-1 genome [11,12]. HBZ-SI is equivalent to the HBZ spliced variant (SPI) initiating in the 3'LTR reported by Cavanagh et al. as an alternative spliced form and to be one of the most abundant HBZ isoforms [13]. Since the spliced and non-spliced HBZ mRNAs have been reported to be detectable in almost all ATL cells tested, HBZ is expected to be closely involved in ATL cell biology corresponding to the late stages of multi-step carcinogenesis of ATL [14].

In this study, to investigate the role of HBZ in the multi-step development of ATL, the quantitative expression levels of HBZ and Tax transcripts were measured by real-time reverse-transcription PCR using HTLV-1-infected cells well characterized by HTLV-1 proviral integration status. Consequently, HBZ transcripts were observed ubiquitously in almost all cells harboring HTLV-1 provirus, and primary ATL cells were characteristic with the very high HBZ transcript levels relative to Tax.

Materials and methods

HTLV-I-infected cells, ATL cells, and cell lines

Blood specimens with cells carrying HTLV-1 provirus from ATL patients and healthy persons were collected in our hospital under the approval of the Research Ethics Committee of our Institute.

According to the status of cytomorphological and clinico-oncological findings, HTLV-1 proviral load and the HTLV-1 proviral integration status were determined by Southern blot analysis and classified into 31 asymptomatic carriers (AC), and 35 patients with ATL. ATL was subtyped according to the JLSG criteria [15]; acute and chronic ATL and ATL in remission. HTLV-1-related cell lines MT1, MT2, HUT102, KK1, KOB, ST1, SO4, OMT, and MT1s were examined in this study. The cell origins of MT1, KK1, KOB, ST1, SO4, and MT1s are ATL cells, whereas those of MT2, HUT102, and OMT are infected normal T-cells. MT1s is a $CD4^{+}$T-cell line derived from MT1 during many passages [16]. All of these cell lines were documented to have 2 or more HTLV-1 proviruses monoclonally integrated into their genomic DNA. KK1, KOB, ST1, OMT, and SO4 were established in our laboratory [17,18].

HTLV-1 infection was demonstrated by a commercial anti-HTLV-1 assay kit (Fujirebio Inc. Tokyo, Japan). In this study, infected cells were defined as non-malignant T-cells randomly integrated with HTLV-1 provirus, while ATL cells were defined as malignant T-cells monoclonally integrated with the provirus.

Methods

DNA and RNA preparation

High molecular weight DNA was extracted from mononuclear blood cells and cell-lines using a QIAmp DNA Blood Mini kit (Qiagen GmbH, Hilden, Germany). Total RNA was extracted using ISOGEN (Nippon Gene, Toyama, Japan). After removing contaminating-genomic DNA using a Message Clean kit, two types of anti-sense cDNA and sense cDNA were synthesized. Sense cDNA was synthesized using Oligo(dT)12–18 Primer and Super-ScriptTM RT (Invitrogen). The first anti-sense strand cDNAs used to amplify both HBZ and HBZ-SI mRNAs were reverse-transcribed using a minus-strand-specific primer, 5'-cccatgtctcaatactacaagaaag-3', in order to avoid contamination of cDNA from the HTLV-1 sense strand genome.

Real-time quantitative RT-PCR for HBZ and HBZ-SI

Real-time RT-PCR was performed using a LightCycler Technology System (Roche Diagnostics) as described previously [11]. Briefly, HBZ or HBZ-SI mRNAs were amplified using anti-sense cDNA as a template and forward and reverse primers specific to the respective transcripts [11]. For the quantification of the amplicons, newly designed

reporter and quencher Hybri-probes common to HBZ and HBZ-SI were used. The reporter and quencher probes were 5'-cagggctgtttcgatgcttgcctgt3'-FITC, and LC-Red-5'-tcatgcccggaggacctgctggt-3'-P, respectively. After 50 cycles, the HBZ or HBZ-SI copy number per 50 ng total RNA was estimated from the standard curves generated by serial dilution of the HBZ and HBZ-SI PCR products derived from ST1 cell line, respectively [11]. Assays were carried out in duplicate and the average value was used as absolute amounts of HBZ mRNA in samples from HTLV-1-infected individuals.

RT-PCR quantification for Tax

The HTLV-1 Tax mRNA load was measured from a template of sense cDNA using the same LightCycler PCR System as described previously [19]. Briefly, PCR amplification was performed according to the manufacturer's instruction using the primers and probes as follows; forward primer, 5'-cccacttcccagggtttggacagag-3'; reverse primer, 5'-cgcgttatcggctcagctctcag-3', reporter probe; 5'-cttttccagaccccggactccg-3'-FITC, and quencher probe, LC-Red-5'-cccaaaacctgtacaccctctg-3'-p. After 50 cycles, the absolute amounts of HTLV-1 Tax mRNA was interpolated from the standard curves generated by the dilution method using Tax plasmids derived from a clone transfected with pGEM Easy Vector containing an amplicon of the Tax. To normalize these results for variability in RNA and cDNA integrity, we monitored abl gene in each sample as an internal control.

SBH and HTLV-I proviral load

Using restriction enzymes of EcoRI and PstI and a digoxigenin-labeled whole HTLV-1 probe, SBH analysis was performed as described previously [20,21]. Visible sharp band(s) from EcoRI digestion and the presence of external band(s) from PstI digestion were considered to be positive, indicating that the cells tested harbor the provirus integrated monoclonally into their genomic DNA. The detection sensitivity was at least 5%.

Next, HTLV-1 proviral load was quantified using a real-time DNA PCR LightCycler Technology System according to our previously described method [22,23]. The primers and probes used were from highly conserved sequences of the Tax gene; sense 5'-cccacttcccagggtttggacagag-3', antisense 5'-cgcgttatcggctcagctctcag-3', reporter probe 5'-cttttccagaccccggactccg-3'-FITC, and quencher probe LC-Red-5'-cccaaaacctgtacaccctctg-3'-P. The sample copy number was estimated by interpolation from the standard curve generated by serial dilution of a Tax-containing plasmid. The detection sensitivity was 10^{-3} (one infected cell relative to 1000 non-infected cells). Normalization was done by using β-globin quantification as an internal control. Assuming one provirus per infected cell (one band in SBH analysis), proviral load was considered to be equivalent to the number of infected cells, namely infected-cell number per 10000 cells = (copy number of Tax)/(copy number of β-globin/2) × 10000.

Statistical analysis

Using the Stat View software, the Mann-Whitney U test or Student's t-test were used to compare data between two groups, and Spearman's rank correlation was used to examine the two groups.

Results

HBZ and spliced HBZ-SI mRNA load in individuals infected with HTLV-I

The HTLV-1 proviral load represents the population of infected cells in blood mononuclear cells when one cell harbors one provirus. Accordingly, we first examined the band status of SBH analysis. Using EcoRI digested DNA samples, SBH analysis revealed one sharp band in 28 ATL samples, two bands in 2 ATL samples, and smeared-bands in 36 AC samples including 5 ATL patients in remission. The samples with two bands were adjusted when the infected cell number was estimated based on the HTLV-1 proviral load. The cell lines used here were also demonstrated to contain multiple proviruses in their genomes, e.g. 8 bands in HUT102 and 2 bands in ST1. Subsequently, the mean value of the HTLV-1 proviral load per 10^4 cells was 316 in ACs, 2739 in ATL patients, and 7600 in cell lines.

HBZs are known to consist of non-spliced and spliced isoforms, HBZ and HBZ-SI, as shown in Figure 1. We firstly evaluated which HBZ isoform was dominant in the 54 samples from sero-positive individuals infected with HTLV-1, including 26 ACs and 28 ATL patients. The median value of un-spliced and spliced HBZ mRNA expression was 0.06×10^3 and 0.2×10^3 in ACs, 1.3×10^3 and 6.0×10^3 in ATL samples, respectively. Of all samples tested, the expression load of HBZ-SI was about 4-fold higher than that of HBZ (mean; 4.9×10^3 vs 1.2×10^3; $p < 0.001$). Accordingly, HBZ-SI was analyzed in this study.

HBZ-SI mRNA load was detected in all but 5 of the 72 samples (3 ACs, one ATL, and one cell line of MT1s and ranged from 0.0 to 6.0×10^5. As shown in Figure 2, the HBZ-SI mRNA load was significantly higher in ATL patients than carriers and lower in ATL patients than cell lines ($p < 0.01$, Mann-Whitney U-test). The relative expression load of the HBZ-SI mRNA among ACs, patients with ATL, and cell lines was 1 : 28 : 350 on average (Table 1). Furthermore, as shown in Figure 3, the HBZ-SI mRNA load was significantly correlated to the infected cell number interpolated from HTLV-1 proviral load analysis. This data reveals that, in order to understand the difference in the expression level of only provirus-positive cells, the absolute amount of HBZ-SI mRNA load should be

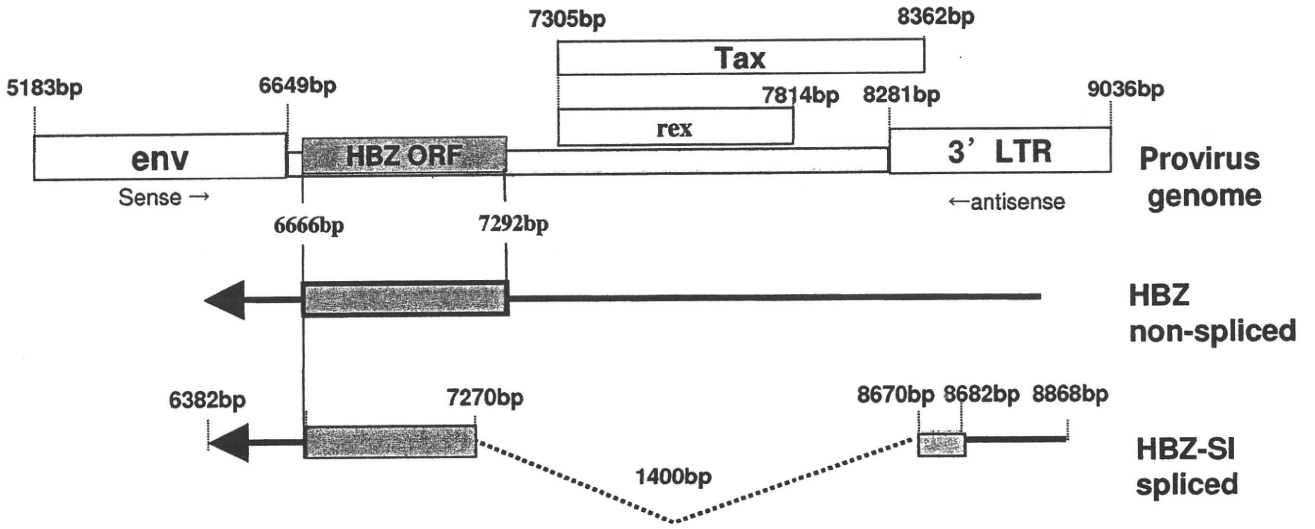

Figure 1
The structure of the HBZ un-spliced (HBZ) and spliced (HBZ-SI) anti-sense transcripts (ATL-YS). HBZ-encoding transcripts initiate in the 3'LTR and are alternatively spliced. The HBZ-SI transcript is about 2.4 kb, consisting of exon 2 corresponding to part of the HBZ ORF (7292 to 6666) and the additional exon 1 (8682 to 8670) at the 3' LTR (11). (ATL-YS; accession no. U19949).

adjusted a value per infected cell number. Accordingly, to adjust the absolute amount of HBZ-SI mRNA load in the samples consisting of a mixture of infected and non-infected cells, the proviral-adjusted HBZ-SI mRNA level (HBZ-SI/HTLV-1) was calculated as follows; (HBZ-SI mRNA load)/(HTLV-1 proviral DNA load) × 10^4. Consequently, the HBZ-SI mRNA expression level after adjustment, as shown in Figure 4, revealed that there was a subtle difference among infected cells, ATL cells, and cell lines. The mean values of the HBZ-SI mRNA load and level before and after adjustment are summarized in Table 1, showing the changes of the relative ratio among ACs (infected cells), ATL patients (ATL cells), and cell lines, from 1 : 28 : 350 to 1 : 6 : 6.

Comparison of HBZ-SI mRNA load with Tax mRNA load in provirus-positive cells

Tax mRNA levels were quantifiable in samples from almost all ATL patients and cell lines, and varied from 0.0 to 10^7. However, there was no correlation between Tax mRNA load and either HBZ-SI mRNA load or proviral load. As shown in Figure 5 and Table 1, although the Tax mRNA load before adjustment was extremely high in only the cell lines, the data after adjustment (Tax/HTLV-1) clarified that ATL cells express Tax at an intensity of 15-fold

Table 1: Comparison of HBZ-SI and Tax mRNA

	ACs	ATL cells	Cell lines	Relative intensity‡ (Acs:ATL : cell lines)
HBZ-SI				
raw data*	0.04 ± 0.06	1.13 ± 1.41	14.01 ± 23.2	(1: 28: 350) §
adjusted*	3.34 ± 4.71	19.82 ± 54.31	19.02 ± 22.2	(1: 6: 6)
Tax				
raw data*	0.009 ± 0.01	0.01 ± 0.02	590.0 ± 989.1	(1: 1: 6600) #
adjusted*	0.9 ± 1.2	0.06 ± 0.01	813.0 ± 1460.0	(1: 1/15: 900) §
HBZ-SI/Tax†	3.7 ± 12.0	330 ± 440&	0.023 ± 0.125	
	low HBZ/low Tax	high HBZ/low Tax	high HBZ/very high Tax	

The proviral adjusted data was calculated by dividing the raw data by HTLV-1 proviral load. Each adjusted value and HBZ-SI/Tax show the characteristic features of the mutual expression patternbetween HBZ-SI and Tax from the viewpoint of relative and absolute transcript levels. * × 104 † ratio ‡ relative expression intensity among three groups §P < 0.01 among three cell types # P < 0.01 among ATL cells and cell lines3); P < 0.01 for ACs and cell lines.

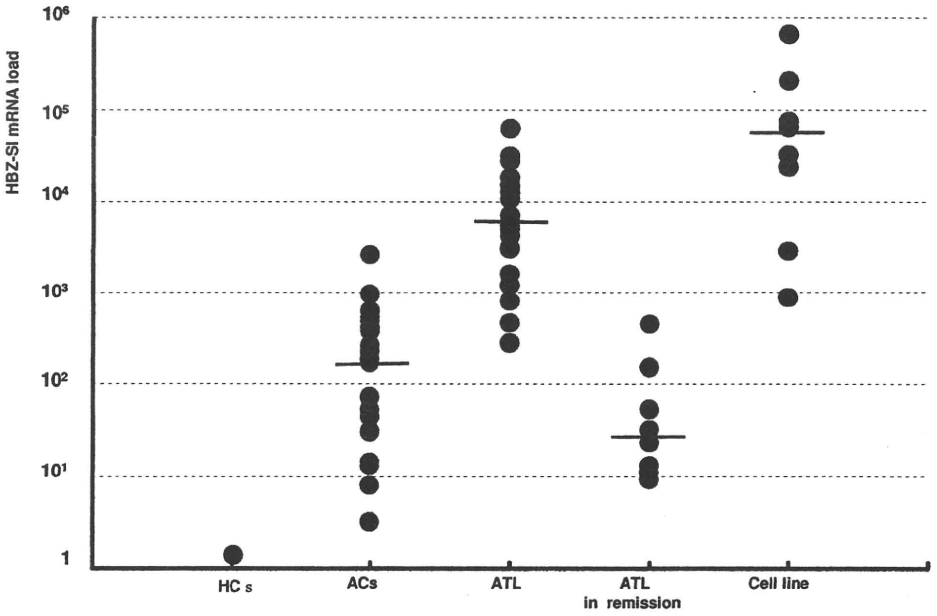

Figure 2
The distribution plots of HBZ-SI mRNA load in different sample groups. Among sero-negative controls, asymptomatic carriers (ACs), patients with ATL, ATL patients in remission, and HTLV-1-related cell lines, there is statistical difference in the median (horizontal bar) among ACs (0.2×10^3) and patients withATL (6.0×10^3) and cell lines (7.5×10^5) ($p < 0.01$).

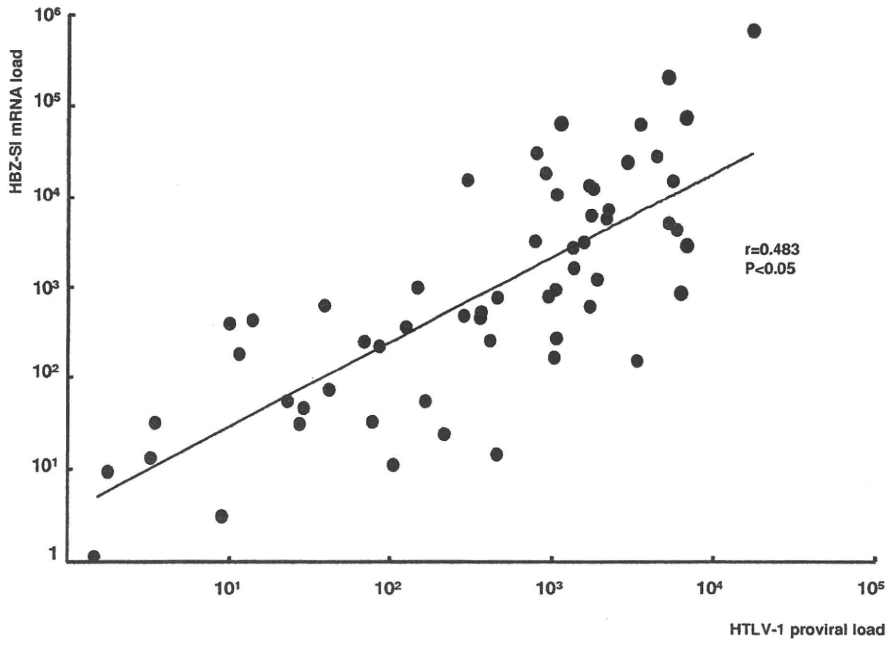

Figure 3
The correlation between HBZ-SI mRNA and HTLV-I proviral loads. The positive correlation between the expression level of HBZ-SI mRNA (Y-axis) and the proviral load (X-axis) equivalent to the infected cell number ($r = 0.483$, $P < 0.05$), indicating that an adjusted HBZ-SI value is indispensable to evaluate the expression level in heterogeneous samples with a mixture of infected and uninfected cells.

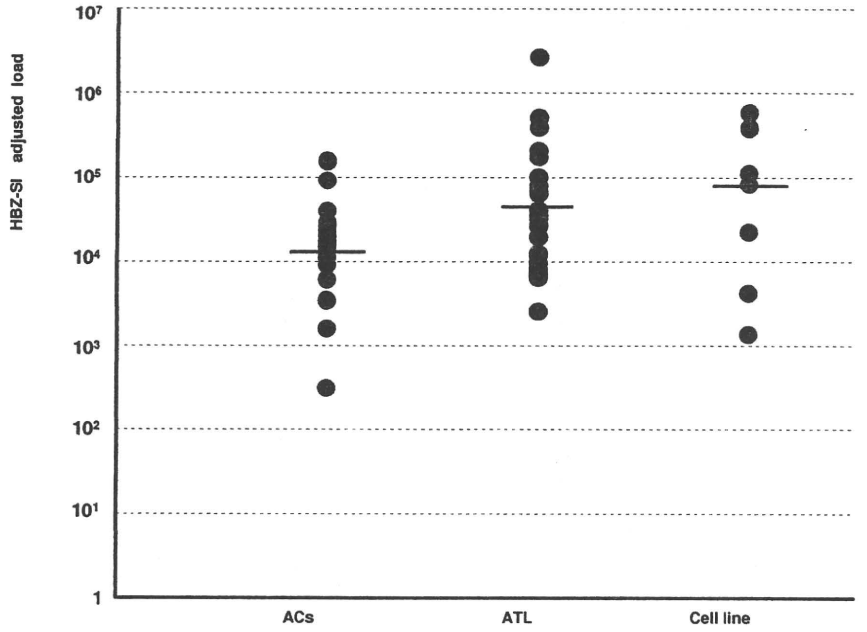

Figure 4
The distribution of HBZ-SI expression level adjusted by HTLV-I proviral load (HBZ-SI/HTLV-I ratio) in each cell group. The relative intensity on average among the three cell types of carriers, ATL cells from patients with ATL, and cell line cells. was about 1:6:6, but was not significantly different.

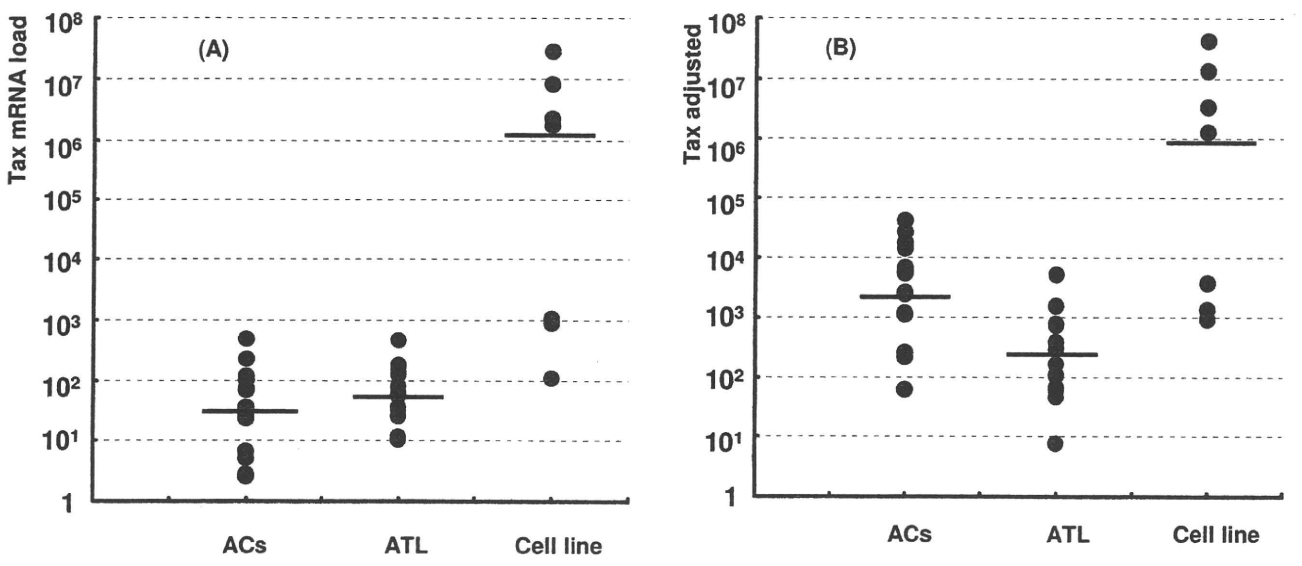

Figure 5
Comparison of Tax mRNA load before (A) and after (B) adjusting by the HTLV-I proviral load. The data before adjustment (A) shows extremely high expression levels in only the cell lines, but that after adjustment shows apparent down-regulation in ATL cells relative to ACs and cell lines.

less than infected cells and approximately 10^4-fold less than ell lines.

Then, to investigate the mutual expression status in the three provirus-positive cell types of non-malignant infected cells, ATL cells, and HTLV-1-related cell lines, the ratio of HBZ-SI/Tax was calculated. The mean ratio of HBZ-SI/Tax was 3.7 in infected cells, 330 in ATL cells, and 0.02 in the cell lines, representing an imbalanced expression between HBZ and Tax in ATL cells and cell lines compared to the base line of the 3.7 in infected cells. This feature is depicted as a twin dot plot of HBZ-SI and Tax loads in Figure 6, showing that each cell type distributes in a specific area implying the characteristic expression status of HBZ and Tax; ATL cells in an area of high HBZ-SI and low Tax, infected cells from ACs in the center area near the ATL cell area, and the majority of cell lines in an area of high Tax and either high or low HBZ. Interestingly, four cell lines (MT1, KK1, SO4, and ST1 in Fig 6 corresponding to the symbols of 1),2),3), and 4)) distributed in the area of high HBZ-SI and low Tax (the ATL cell area) all originated from an ATL cell clone, while three other lines (OMT, MT2, and HUT102 in Fig 6; 5),7), and 8)) out of 4 distributed in the area of high-Tax and either high or low-HBZ-SI were derived from infected cells.

Since loss of HBZ-SI or Tax transcripts in MT1s and underestimation of proviral copy number in KK1 was observed in this study, we examined the genomic structure of the provirus by DNA PCR amplifying between nucleotides (nt) 6461 to 8853 including the region of the HBZ gene. Interestingly, as shown in panel B of Figure 7, the expected wild-type band of 2393 bp was undetectable for KK1 and MT1s, whereas MT1s, as shown in panel C, was negative for the full-length cDNA band (994 bp) derived from HBZ-SI anti-sense transcripts. These findings suggest that loss of HBZ and underestimation of the HTLV-1 proviral load could be in part explained by this genomic alteration.

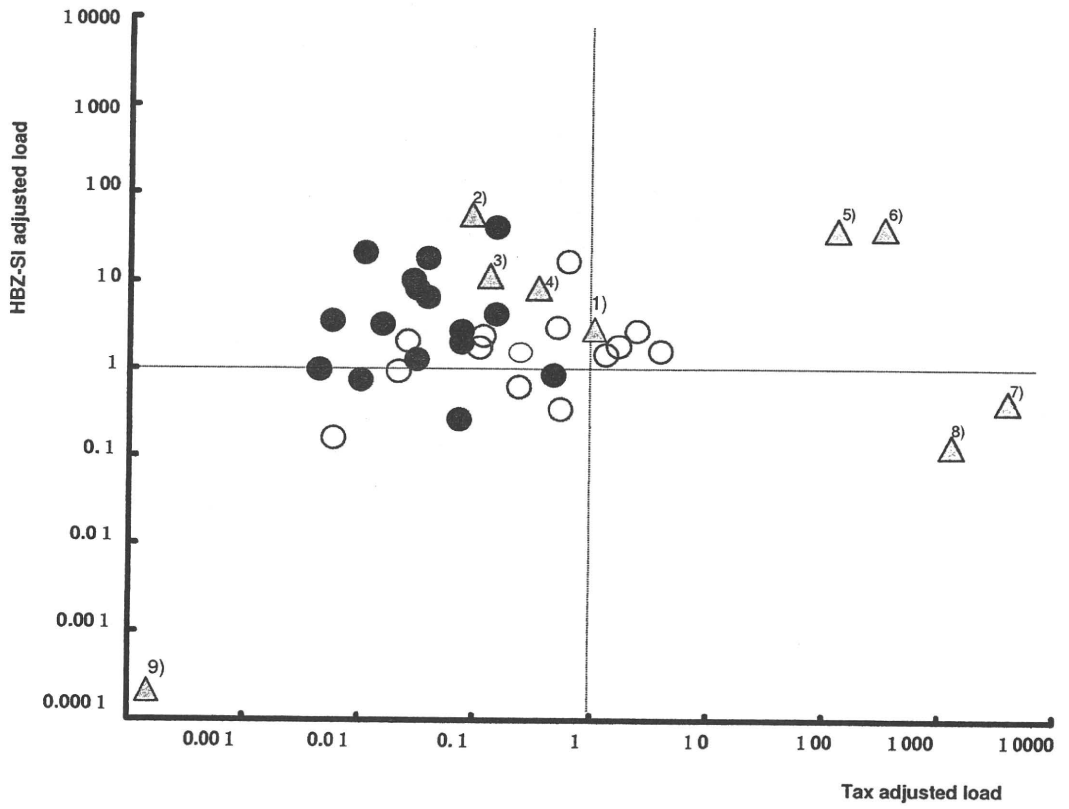

Figure 6

Dot plot graph for the proviral-adjusted HBZ-SI mRNA load and the proviral-adjusted Tax mRNA load. Each plot (Y-axis; HBZ-SI/HTLV-I ratio, and X-axis; tax/HTLV-I ratio) reveals the characteristic expression balance between HBZ and Tax in each cell type. ATL samples and AC samples are clustered in a low tax and high HBZ-SI area and in a central area, respectively. Of HTLV-I-related cell lines, there are two distribution types, one is ATL sample type with high HBZ-SI and low Tax, and another is a type with high Tax and either high or low HBZ-SI. Open circle; infected cells of ACs, closed circle; ATL cells, solid triangle; cell lines. 1); MT-1, 2); KK1, 3); SO4, 4); ST1, 5); OMT, 6); KOB, 7);MT2, 8); Hut102, and 9);MT1s.

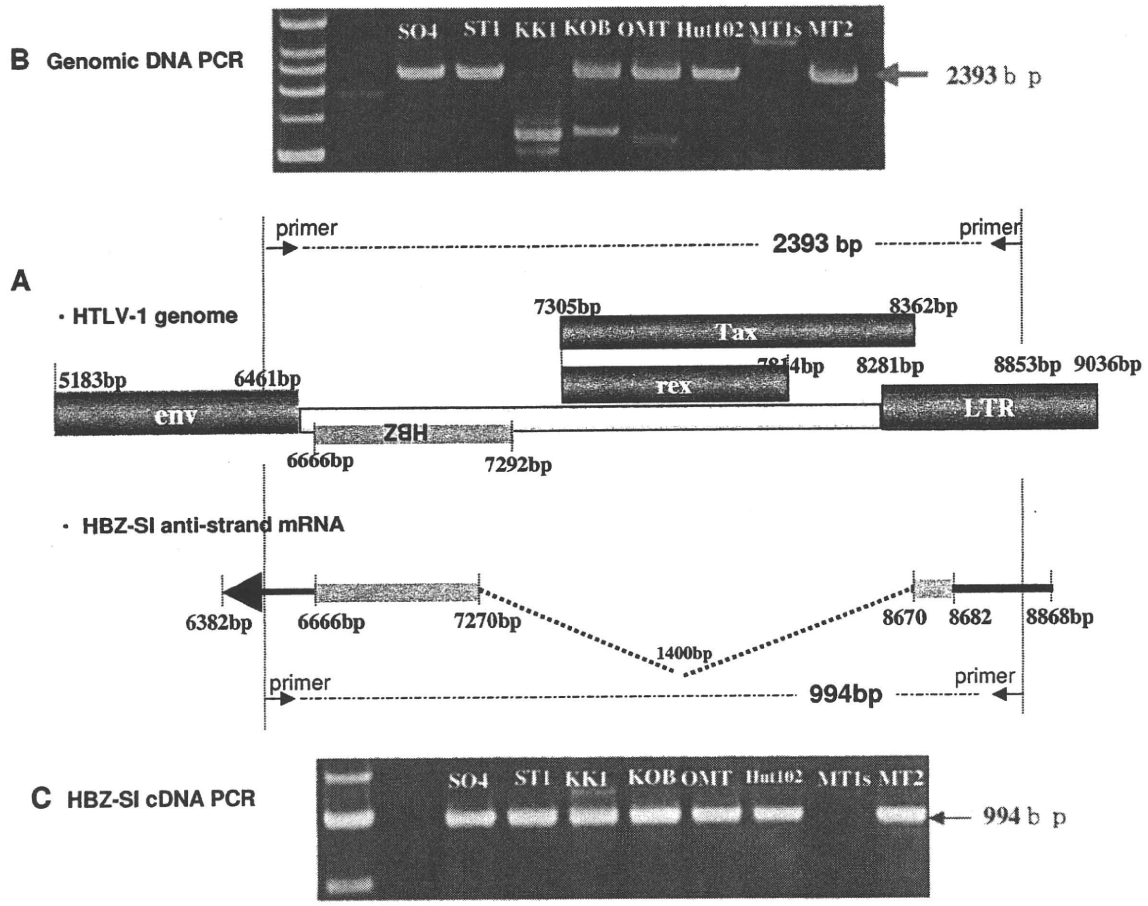

Figure 7
DNA and RT-PCR analyses for the pX region including HBZ gene and for anti-sense transcript, HBZ-SI. (A): Schematic representation of HTLV-I genome at the position of the HBZ antisense ORF, the initiation site of the transcript, and the primer-setting positions. (B): PCR product band of the genomic region corresponding to the full-length antisense transcript. No band of the expected 2393 bp size was observed in the MT1s lane and an aberrant band was detected in the KK1 lane. (C): RT-PCR product band of anti-sense products of HBZ-SI. No band corresponding to the transcript was observed in MT1s, and only one band was visible in the other samples.

Discussion

Many studies have indicated that Tax is likely to be a central player in the induction of ATL. However, nobody has answered the paradoxical question why T-cell transformation and clonal proliferation of ATL cells is associated with a Tax-low or -negative phenotype. HBZ, a novel viral factor encoded from the minus-strand RNA of HTLV-1, is expected to play an important role in HTLV-1 biology by counteracting the action of Tax. Indeed, HBZ has been shown to interact with the cellular transcription factor CREB to inhibit HTLV-1 transcription [24]. However, there has not yet been a comprehensive study regarding the mutual expression profiles of HBZ and Tax in HTLV-1-provirus-positive cells, including infected cells, primary ATL cells, and HTLV-1-related cell lines.

This study demonstrated a ubiquitous expression of HBZ isoforms, mainly the spliced isoform of HBZ-SI, in almost all provirus-positive cells. Furthermore, in contrast to Tax, up-regulation of HBZ was characteristic of primary ATL cells, although the increase in level was subtle. These results were supported by previous studies describing that HBZ mRNA is expressed in all fresh ATL cells and HTLV-1 cell lines [11,12,25], but no quantitative observations have been reported in a large scale study. First of all, we evaluated the difference in the expression intensity between unspliced HBZ and spliced HBZ-SI (corresponding to HBZ (SP1)). Consistent with the data from a small range of samples by Cavanagh et al. [13], our results in a large range of samples clarified that HBZ-SI is the most

abundant isoform, about 4-fold higher than unspliced HBZ.

Interestingly, HBZ-SI mRNA was detectable in samples from almost ACs and ATL patients. Furthermore, the HBZ-SI mRNA load was significantly correlated with the HTLV-proviral load, but not the Tax mRNA load. On the other hand, although Tax mRNA was also subtly detectable in blood samples from ACs and patients with ATL, it was not correlated with the HTLV-1 proviral load. These results indicate that the expression profile of HBZ is different from Tax, namely HBZ is near-equally expressed by all provirus-positive cells, while Tax levels are variable and can be actively up-regulated when necessary. In other words, the absolute amount of HBZ-SI mRNA load is dependent on the total of infected cells estimated by the proviral load within samples consisting of a mixture of infected and non-infected cells. Accordingly, in order to compare the expression intensity per provirus-positive cells only, it is reasonable to adjust by dividing the HBZ-SI mRNA load by the proviral copy number estimated by the HTLV-1 proviral load [26]. Actually, although the data before adjustment was generally low in ACs and patients with ATL, the adjusted data elucidated that there are no or only subtle differences in HBZ-SI expression level among infected cells, primary ATL cells, and cell lines. In particular, the relative HBZ-SI intensity of primary ATL cells and cell lines to infected cells changed from 1 : 28 : 350 before to 1 : 6 : 6 after adjustment. This up-regulation of 6-fold higher levels in primary ATL cells than infected cells is noteworthy in implication of HBZ for oncogenesis because it has been suggested that HBZ may play an important role in HTLV-1 biology by counteracting the action of Tax. Therefore, we examined the mutual expression profiles of HBZ and Tax. Our quantification analysis showed that infected cells express Tax at low levels, while primary ATL cells down-regulate Tax expression levels by 15-fold, and cell lines highly up-regulate Tax levels by 900-fold (1 : 1/15 : 900). The ratio of HBZ-SI against Tax was 4 in infected cells, 330 in primary ATL cells, and 0.02 in cell lines. Our data of the 0.02 ratio in cell lines is similar to previous data that HBZ mRNA levels are 20- to 50-fold lower (0.02) than Tax mRNA levels [12,14,27]. All of these findings indicate a characteristic imbalanced expression feature of high-HBZ and low-Tax in primary ATL cells and high-HBZ and very high-Tax in cell lines compared with a standard expression of low-HBZ and low-Tax in infected cells.

What does the difference in the mutual expression patterns, such as low-HBZ and low-Tax in infected cells, high-HBZ and no or subtle-Tax in primary ATL cells, and variable high or low HBZ and Tax in cell lines mean? Currently, only the role of Tax is stressed for oncogenic pathogenesis of HTLV-1, so the co-operative occurrence of up-regulated HBZ and down-regulated Tax may be closely associated with the oncogenic process in the early stage and with the persistent maintenance of malignancy in the late stage. Interestingly, recent reports on HBZs encoded from the minus strand of HTLV-1 seem to be providing a new insight in the current models of Tax-centered HTLV-1 pathogenesis, such as ATL oncogenesis and viral replication. In particular, the bimodal function of HBZs is of interest, in which the HBZ protein suppresses Tax transactivation of E2F1 and the HBZ mRNA promotes T-cell proliferation [12,25]. Furthermore, activation of telomerase is a critical and late event in tumor progression, HBZ also was reported to have the potential to activate telomerase through transcriptional up-regulation of hTERT by interaction with JunD and to contribute the development and maintenance of the ATL development [28]. Thus, since HBZs and Tax are thought to mutually interact with each other in the process of the multi-step oncogenesis, the imbalanced expression of HBZ and Tax in ATL cells can lead to better understand of ATL cell biology.

Another important point of this study is a mutual correlation of Tax and HBZ mRNA expression level in HTLV-1-associated cell lines. Although Tax mRNA is generally said to be low or negative in all ATL cells and extremely high in cell lines, our Tax mRNA quantification clarified that Tax mRNA was detectable in almost ATL cells at the intensity of approximately 10^4 fold less than that in MT2 cells, which is consistent with previous results as reported by Furukawa et al. [29]. In contrast, cell lines are known to have high levels of Tax mRNA, but our quantitative results showed that there are two types of Tax expression pattern; low Tax and high HBZ (ATL cell type) and high Tax and low (rarely high) HBZ (non-ATL cell type). This inverse correlation of Tax and HBZ expression may be explained by the HBZ function to control HTLV-1 replication as mentioned above (29). However, the existence of exceptional cases with both high Tax and HBZ expression suggests that HBZ is not everything to control Tax. Additionally, the mutual characteristic expression from cell lines appeared to correlate with its cell origin. Namely, the cell origin of cell lines having the ATL cell type of HBZ and Tax expression was a leukemic clone, while that of the non-ATL cell type was derived from HTLV-1-infected non-leukemic cells. That is, HTLV-1-related cell lines preserve the essential Tax and HBZ expression features of the original cell type.

KK1 and MT1s were found to harbor defective proviruses involving the pX/HBZ gene region, probably resulting in the loss of tax and HBZ mRNA expression in the MT1s. Despite the absence of HBZ, the cells have immortalized and survived for many generations, suggesting the possibility that HBZ may not be required in ATL cells, at least in cell lines.

In conclusion, our study provides better understanding of multi-step leukomogenesis in ATL through the characteristic expression of HBZ isoforms. Among the isoforms of HBZ, HBZ-SI is dominant over non-spliced HBZ. HBZ-SI is constantly and ubiquitously expressed in all cells harboring HTLV-1 provirus and is more highly expressed in ATL cells than in infected cells. To address ATL cell pathology induced by viral factors, it is of importance to evaluate simultaneously Tax and HBZ mRNA levels and proviral load.

Abbreviations

HBZ: HTLV-1 basic zipper factor; SBH: Southern blot hybridization; PCR: polymerase chain reaction; AC: asymptomatic carriers; HTLV-1: human T-cell leukemia virus type-1; ATL: adult T-cell leukemia.

Competing interests

The authors declare that they have no competing interests.

Authors' contributions

TU designed the study, and performed the analysis. KY, KT, KM and HH recruited and monitored the subjects. YY provided the cell lines. SK made substantial contributions to the conception and design of the study, wrote and drafted the manuscript, and contributed to data interpretation.

Acknowledgements

We thank Prof Toshiki Watanabe and Dr Kazunari Yamaguchi, core members of the Joint Study on Predisposing Factors of ATL Development, in conducting this study. This study was supported financially by Japan Society for the Promotion of Science (No 17390165).

References

1. Uchiyama T, Yodoi J, Sagawa K, Takatsuki K, Uchino H: **Adult T-cell leukemia: clinical and hematologic features of 16 cases.** *Blood* 1977, **50**:481-92.
2. Hinuma Y, Nagata K, Hanaoka M, Nakai M, Matsumoto T, Kinoshita KI, Shirakawa S, Miyoshi I: **Adult T-cell leukemia: antigen in an ATL cell line and detection of antibodies to the antigen in human sera.** *Proc Natl Acad Sci USA* 1981, **78**:6476-6480.
3. Poiesz BJ, Ruscetti FW, Gazdar AF, Bunn PA, Minna JD, Gallo RC: **Detection and isolation of type C retrovirus particles from fresh and cultured lymphocytes of a patient with cutaneous T-cell lymphoma.** *Proc Natl Acad Sci USA* 1980, **77**:7415-7419.
4. Peloponese JM Jr, Kinjo T, Jeang KT: **Human T-cell leukemia virus type 1 Tax and cellular transformation.** *Int J Hematol* 2007, **86**:101-106.
5. Yasunaga J, Matsuoka M: **Leukaemogenic mechanism of human T-cell leukaemia virus type I.** *Rev Med Virol* 2007, **17**:301-311.
6. Giam CZ, Jeang KT: **HTLV-1 Tax and adult T-cell leukemia.** *Front Biosci* 2007, **12**:1496-1507.
7. Nicot C, Harrod RL, Ciminale V, Franchini G: **Human T-cell leukemia/lymphoma virus type 1 nonstructural genes and their functions.** *Oncogene* 2005, **24**:6026-6034.
8. Matsuoka M: **Human T-cell leukemia virus type I (HTLV-I) infection and the onset of adult T-cell leukemia (ATL).** *Retrovirology* 2005, **2**:27.
9. Larocca D, Chao LA, Seto MH, Brunck TK: **Human T-cell leukemia virus minus strand transcription in infected T-cells.** *Biochem Biophys Res Commun* 1989, **163**:1006-10013.
10. Gaudray G, Gachon F, Basbous J, Biard-Piechaczyk M, Devaux C, Mesnard JM: **The complementary strand of the human T-cell leukemia virus type 1 RNA genome encodes a bZIP transcription factor that down-regulates viral transcription.** *J Virol* 2002, **76**:12813-12822.
11. Murata K, Hayashibara T, Sugahara K, Uemura A, Yamaguchi T, Harasawa H, Hasegawa H, Tsuruda K, Okazaki T, Koji T, Miyanishi T, Yamada Y, Kamihira S: **A novel altemative splicing isoform of human T-cell leukemia virus type 1 bZIP factor (HBZ-SI) targets distinct subnuclear localization.** *J Virol* 2006, **80**:2495-2505.
12. Satou Y, Yasunaga J, Yoshida M, Matsuoka M: **HTLV-I basic leucine zipper factor gene mRNA supports proliferation of adult T cell leukemia cells.** *Proc Natl Acad Sci USA* 2006, **103**:720-725.
13. Cavanagh MH, Landry S, Audet B, Arpin-André C, Hivin P, Paré ME, Thête J, Wattel E, Marriott SJ, Mesnard JM, Barbeau B: **HTLV-I antisense transcripts initiating in the 3'LTR are alternatively spliced and polyadenylated.** *Retrovirology* 2006, **3**:15.
14. Mesnard JM, Barbeau B, Devaux C: **HBZ, a new important player in the mystery of adult T-cell leukemia.** *Blood* 2006, **108**:3979-3982.
15. Shimoyama M: **Diagnostic criteria and classification of clinical subtypes of adult T-cell leukaemia-lymphoma. A report from the Lymphoma Study Group (1984–87).** *Br J Haematol* 1991, **79**:428-437.
16. Miyoshi I, Kubonishi I, Yoshimoto S, Akagi T, Ohtsuki Y, Shiraishi Y, Nagara K, Hinuma Y: **Type C virus particles in a cord T-cell line derived by co-cultivating normal human cord leukocytes and human leukaemic T-cells.** *Nature* 1981, **294**:770-771.
17. Yamada Y, Sugawara K, Hata T, Tsuruta K, Moriuchi R, Maeda T, Atogami S, Murata K, Fujimoto K, Kohno T, Tsukasaki K, Tomonaga M, Hirakata Y, Kamihira S: **Interleukin-15 (IL-15) can replace the IL-2 signal in IL-2-dependent adult T-cell leukemia (ATL) cell lines: expression of IL-15 receptor alpha on ATL cells.** *Blood* 1998, **91**:4265-4272.
18. Maeda T, Yamada Y, Moriuchi R, Sugahara K, Tsuruda K, Joh T, Atogami S, Tsukasaki K, Tomonaga M, Kamihira S: **Fas gene mutation in the progression of adult T cell leukemia.** *J Exp Med* 1999, **189**:1063-1071.
19. Hasegawa H, Yamada Y, Harasawa H, Tsuji T, Murata K, Sugahara K, Tsuruda K, Ikeda S, Imaizumi Y, Tomonaga M, Masuda M, Takasu N, Kamihira S: **Sensitivity of adult T-cell leukaemia lymphoma cells to tumour necrosis factor-related apoptosis-inducing ligand.** *Br J Haematol* 2005, **128**:253-265.
20. Kamihira S, Sugahara K, Tsuruda K, Minami S, Uemura A, Akamatsu N, Nagai H, Murata K, Hasegawa H, Hirakata Y, Takasaki Y, Tsukasaki K, Yamada Y: **Proviral status of HTLV-I integrated into the host genomic DNA of adult T-cell leukemia cells.** *Clin Lab Haematol* 2005, **27**:235-241.
21. Uemura A, Sugahara K, Nagai H, Murata K, Hasegawa H, Hirakata Y, Tsukasaki K, Yamada Y, Kamihira S: **An ATL cell line with an IgH pseudo-rearranged band pattern by southern blotting: a pitfall of genetic diagnosis.** *Lab Hematol* 2005, **11**:8-13.
22. Kamihira S, Dateki N, Sugahara K, Hayashi T, Harasawa H, Minami S, Hirakata Y, Yamada Y: **Significance of HTLV-I proviral load quantification by real-time PCR as asurrogate marker for HTLV-I-infected cell count.** *Clin Lab Haematol* 2003, **25**:111-117.
23. Kamihira S, Dateki N, Sugahara K, Yamada Y, Tomonaga M, Maeda T, Tahara M: **Real-time polymerase chain reaction for quantification of HTLV-I proviral load: application for analyzing aberrant integration of the proviral DNA in adult T-cell leukemia.** *Int J Hematol* 2000, **72**:79-84.
24. Lemasson I, Lewis MR, Polakowski N, Hivin P, Vavanagh M-H, Thebault S, Barbeau B, Nyborg JK, Mesnard J-M: **HTLV-I bZIP protein interacts with the cellular transcription factor CREB to inhibit HTLV-I transcription.** *J Virol* 2007, **81**:1543-1553.
25. Satou Y, Matsuoka M: **Implication of the HTLV-I bZIP factor gene in the leukemogenesis of adult T-cell leukemia.** *Int J Hematol* 2007, **86**:107-112.
26. Yamano Y, Nagai M, Brennan M, Mora CA, Soldan SS, Tomaru U, Takenouchi N, Izumo S, Osame M, Jacobson S: **Correlation of human T-cell lymphotropic virus type 1 (HTLV-1) mRNA with proviral DNA load, virus-specific CD8(+) T cells, and disease severity in HTLV-1-associated myelopathy (HAM/TSP).** *Blood* 2002, **99**:88-94.
27. Arnold J, Yamamoto B, Li M, Phipps AJ, Younis I, Lairmore MD, Green P: **Enhancement of infectivity and persistence in vivo by HBZ,**

a natural antisense coded protein of HTLV-1. *Blood* 2006, **107**:3976-3982.
28. Kuhlmann A-S, Villaudy J, Gazzolo L, Castellazzi M, Mesnard J-M, Duc Dodon M: **HTLV-1 HBZ cooperates with JunD to enhance transcription of the human telomerase transcriptase gene (hTERT).** *Retrovirology* 2007, **4**:92.
29. Furukawa Y, Osame M, Kubota R, Tara M, Yoshida M: **Human T-cell leukemia virus type-1 (HTLV-1) Tax is expressed at the same level in infected cells of HTLV-1-associated myelopathy or tropical spastic paraparesis patients as in asymptomatic carriers but at a lower level in adult T-cell leukemia cells.** *Blood* 1995, **85**:1865-1870.

Available online at www.sciencedirect.com
ScienceDirect
Cancer Letters 271 (2008) 167–177
CANCER Letters
www.elsevier.com/locate/canlet

Activation of complement system in adult T-cell leukemia (ATL) occurs mainly through lectin pathway: A serum proteomic approach using mass spectrometry

Yo-ichi Ishida [a,*], Kiyoshi Yamashita [b], Hidenori Sasaki [b], Ichirou Takajou [a,c], Yoko Kubuki [d], Kazuhiro Morishita [e], Hirohito Tsubouchi [f], Akihiko Okayama [a,c]

[a] *Miyazaki Prefectural Industrial Support Foundation, 16500-2, Higashi-Kaminaka, Sadowara-cho, Miyazaki, 880-0303, Japan*
[b] *Division of Gastroenterology and Hematology, University of Miyazaki, 5200, Kihara, Kiyotake, Miyazaki, 889-1692, Japan*
[c] *Division of Rheumatology, Infectious Diseases, and Laboratory Medicine, Department of Internal Medicine, Faculty of Medicine, University of Miyazaki, 5200, Kihara, Kiyotake, Miyazaki, 889-1692, Japan*
[d] *Blood Transfusion Unit, University of Miyazaki Hospital, University of Miyazaki, 5200, Kihara, Kiyotake, Miyazaki, 889-1692, Japan*
[e] *Division of Tumor and Cellular Biochemistry, Department of Medical Sciences, Faculty of Medicine, University of Miyazaki, 5200, Kihara, Kiyotake, Miyazaki, 889-1692, Japan*
[f] *Digestive Disease and Lifestyle-related Disease Health Research, Human and Environmental Sciences, Kagoshima University Graduate School of Medicine and Dental Sciences, 8-35-1, Sakuragaoka, Kagoshima, 890-8544, Japan*

Received 23 March 2008; received in revised form 29 May 2008; accepted 2 June 2008

Abstract

Adult T-cell leukemia (ATL) is a fatal malignancy caused by infection with human T lymphotropic virus type-1 (HTLV-1). To search for a new biomarker of ATL, we analyzed sera from ATL patients using ProteinChip arrays. The spectral comparison of ATL patients with HTLV-1 carriers and healthy volunteers showed that the intensities of five peaks (1779, 1866, 2022, 4467, and 8930 m/z) were significantly increased in ATL, while those of four peaks (4067, 4151, 8130, and 8597 m/z) were decreased. From these differentially expressed peaks, we chose peaks of 1779, 1866, and 2022 m/z as biomarker candidates of ATL. MS/MS ion search using tandem mass spectrometry and immunoprecipitation assay using anti-C3 antibody showed that factors derived from these candidate peaks were identified as C3f, which is a component of the complement system and a fragment of complement C3. These results indicate that the complement system was activated in ATL. Further analysis of markers specific to the activation pathways (classical, alternative, and lectin pathways) in the complement system showed that the serum concentration of the marker of the lectin pathway was significantly higher in ATL patients. These results suggest that activation of the complement system in ATL occurs mainly through the lectin pathway.

Keywords: ATL; ProteinChip array; C3f; Complement system; Lectin pathway

* Corresponding author. Tel.: +81 985 74 4007; fax: +81 985 74 4033.
E-mail address: ishida@mi-create.jp (Y. Ishida).

0304-3835/$ - see front matter © 2008 Elsevier Ireland Ltd. All rights reserved.
doi:10.1016/j.canlet.2008.06.004

1. Introduction

Adult T-cell leukemia (ATL) is a fatal malignancy caused by infection with human T lymphotropic virus type-1 (HTLV-1) [1,2]. About 2–5% of HTLV-1 carriers develop ATL after a long latent period (30–50 years) [3]. During this long latency, it has been assumed that various abnormalities, such as the enhanced expression of genes/proteins of the virus and/or host cells, accumulate in HTLV-1-infected T-cells. The infected cells then escape from the immune system and a fully malignant cell (ATL cell) appears [4]. The *tax* and *HTLV-1 bZIP factor (HBZ)*, which are viral-specific genes, have been suggested to be associated with ATL development [4,5]; however, the developmental mechanism and the response of the host immune system against ATL cells are not fully understood.

Proteomic analysis is a powerful tool for the discovery of new biomarkers and investigation into cancer development [6,7]. ProteinChip array, coupled with surface-enhanced laser desorption/ionization time-of-flight mass spectrometry (SELDI-TOF-MS; Bio-Rad Laboratories, Inc., CA, USA), has been successfully applied to diagnose various malignancies, such as ovarian cancer and gastric cancer [8,9]. In that method, proteins/peptides in the biological fluid are captured by a variety of arrays with different chromatography surfaces, for example, a cationic exchanger. Captured proteins/peptides are then analyzed by SELDI-TOF-MS, generating a spectral map depicting the molecular weight (mass/charge; m/z) and relative concentration (peak intensity) of each protein/peptide. By comparing the spectral maps between disease and non-disease status, disease-specific peaks are detected [6,7]. Furthermore, factors derived from these peaks can be identified by MS/MS ion search, using tandem MS, such as matrix-assisted laser desorption/ionization (MALDI)-TOF-TOF-MS [10]. Using proteomic analysis, alpha trypsin inhibitor and haploglobin-2 have been reported to be identified as markers of ATL [11].

We have been studying the developmental mechanisms of ATL and hepatocellular carcinoma (HCC), which are both human viral malignancies [12–17]. In a previous report, we developed an early diagnostic method of HCC using six peaks detected in ProteinChip array analyses and demonstrated that this method is useful for the early detection and prediction of HCC [18]. Thus, in this study, we focused on ATL. To search for new biomarkers of ATL, we analyzed sera from ATL patients using proteomic tools. Our experiments demonstrated that the expression of C3f, which is a component of the complement system, was markedly increased in ATL.

A few studies have reported the relationship of the complement system to other HTLV-1-associated disease and the virus [19–21]; however, the role of the complement system in ATL is still unknown. Here, we further investigated its activating mechanism in ATL, focusing on three distinct pathways: classical, alternative, and lectin pathways [22–24]. From the expression analysis of markers specific to these pathways, it was suggested that activation of the complement system in ATL occurred mainly through the lectin pathway.

2. Materials and methods

2.1. Serum samples

Serum samples were obtained from 20 patients with ATL, 20 HTLV-1 carriers, and 16 healthy volunteers without HTLV-1 infection. The diagnosis was performed at Medical College Hospital, University of Miyazaki; the diagnosis of ATL was made on the basis of clinical features, hematologic characteristics, and serum antibodies against HTLV-1 antigens. Using Shimoyama criteria, 16 and 4 ATL patients were diagnosed with the acute type and lymphoma type, respectively [25]. Serum samples of HTLV-1 carriers and healthy individuals were obtained in the Miyazaki Cohort Study, which was established in 1984 for the primary purpose of investigating the natural history of HTLV-1 infection [26]. Informed consent was obtained from all study subjects. All serum samples were stored at −80 ℃ until analysis. The study protocol was approved by the Institutional Review Boards at the University of Miyazaki and the Miyazaki Prefectural Industrial Support Foundation.

2.2. Expression profiling of serum proteins/peptides

Serum samples were subjected to ProteinChip arrays coupled with SELDI-TOF-MS. Namely, 5 μl of serum was pretreated with 45 μl of phosphate-buffered saline (PBS; NaCl 8 g/l, KCl 0.2 g/l, $Na_2HPO_4 \cdot 12H_2O$ 2.9 g/l, KH_2PO_4 0.2 g/l) for 10 min on ice, and diluted with 200 μl of 50 mM sodium acetate (pH 5.5). Then, 100 μl of the diluted

serum was added to the CM10 ProteinChip arrays (Bio-Rad Laboratories, Inc.) with the aid of a Bioprocessor (Bio-Rad Laboratories, Inc.) and incubated for 30 min at room temperature with gentle shaking. After washing with 50 mM sodium acetate (pH 5.5) and water, arrays were air-dried. Each spot was then treated twice with 0.5 μl of 50% saturated solution of α-cyano-4-hydroxycinnamic acid (CHCA; Bruker Daltonics, Inc., MA, USA) and allowed to air-dry.

Arrays were analyzed using a ProteinChip reader (ProteinChip Biology Systems II) (Bio-Rad Laboratories, Inc.). Spectra were generated by laser shots collected in positive mode. Spectra were collected by the accumulation of 65 shots at laser intensity 180 and detector sensitivity 8. For mass accuracy calibration according to the manufacturer's instructions, 0.5 μl of a mixture of mass standard calibration peptides (All-in-one Peptide Standard; Bio-Rad Laboratories, Inc.) was applied in a single spot on the normal phase ProteinChip arrays (NP20) (Bio-Rad Laboratories, Inc.) followed by two applications of 1.0 μl of 50% saturated CHCA. The mass-to-charge ratio (m/z) of each peptide captured on the array surface was determined according to externally calibrated standards.

Peak detection was performed using Ciphergen ProteinChip Software, version 3.0.2 (Bio-Rad Laboratories, Inc.). Spectra between 800 and 10,000 m/z were selected for analysis. After baseline subtraction, spectra were normalized to total ion current intensity. Automatic peak detection was performed in the range of 1000–10,000 m/z, using peak auto-detection set to cluster, a first-pass signal/noise ratio of 7, a minimal peak threshold of 30% for all spectra, and a cluster mass window of 0.3% mass. Peak intensity in spectra and statistical differences were determined using Biomarker Wizard Software (Bio-Rad Laboratories, Inc.). Values shown are the means ± standard deviation (SD) or standard error (SE). Statistical differences were determined by the Mann–Whitney U test. Values of $P < 0.001$ were considered significant.

2.3. Identification of peptides by MS/MS ion search

Peptides derived from peaks were identified by MS/MS ion search using tandem MS [10]. CM10 ProteinChip arrays were mounted on Special Target (Bruker Daltonics, Inc.) and then measured using MALDI-TOF-TOF-MS, Autoflex II TOF/TOF (Bruker Daltonics, Inc.). MS/MS fragmentation generated a set of parent ions and fragment ions. The data set was entered in a mass spectrometry database search engine, Mascot (http://www.matrixscience.com/), to find the closest match with known proteins/peptides registered in the database from the National Center for Biotechnology Information (NCBI) web site.

2.4. Immunoprecipitation assay

Ten microliters of serum from an ATL patient was diluted with 40 μl of PBS, treated with goat antiserum against C3 (anti-C3 polyclonal antibody) or goat serum (1.4 mg/ml) (MP Biomedicals Inc., OH, USA), and incubated for 1 h at 4 ℃. Then 10% [vol/vol] protein A-Sepharose CL-4B (GE Healthcare Bio-Sciences Corp., NJ, USA) was added and incubated for 1 h at 4 ℃ with gentle shaking. After centrifugation at 400g, supernatants were harvested. Immunoprecipitates bound to Sepharose beads were washed 5 times with PBS and then eluted by treatment with 30 μl of 50% [vol/vol] acetonitrile. Harvested supernatants or immunoprecipitates were diluted 1:4 in 50 mM sodium acetate (pH 5.5), treated with the CM10 ProteinChip arrays, and then analyzed using a ProteinChip reader, as described above.

2.5. Analysis of components of the complement system

The concentration of iC3b, circulating immunocomplex (CIC), b-fragment of factor B (Bb), and functional mannose-binding lectin (MBL)/MBL-associated serine protease 2 (MASP-2) in serum was examined using commercially available kits. Namely, iC3b, CIC, Bb, and functional MBL/MASP-2 were analyzed using the iC3b Enzyme Immunoassay kit (Quidel Co., CA, USA), C1q Solid-phase Enzyme Immunoassay (SRL Co., Tokyo, Japan), Bb Fragment Enzyme Immunoassay kit (Quidel Co.), and Hbt human MBL-C4 activation complex test kit (Hucult Biotechnology, Uden, Netherlands), respectively. All standards and serum samples were measured in duplicate. Values shown are the means ± SE. Statistical differences were determined by the Mann–Whitney U test. Values of $P < 0.05$ were considered significant.

3. Results

3.1. Peaks of 1779, 1866, and 2022 m/z as biomarker candidates of ATL

To search for biomarkers of ATL, we performed serum proteomic analysis using ProteinChip arrays. First, the expression profiles of serum proteins/peptides in ATL patients were compared with those in HTLV-1 carriers and healthy volunteers. As shown in Fig. 1, the spectra of ATL patients (A) were markedly different from those of HTLV-1 carriers (B) and healthy volunteers (C). In the ranges of 1700–2100, 3500–5000, and 7500–10000 m/z (asterisks in Fig. 1), the intensities of several peaks appeared to be increased or decreased in ATL patients; however, no difference was seen between HTLV-1 carriers (Fig. 1B) and healthy volunteers (Fig. 1C). For further analyses of detected spectra, quantitative analysis of detected peaks was performed (Table 1). In ATL patients, the intensities of five peaks (1779, 1866, 2022, 4467, and 8930 m/z) were significantly increased as compared with HTLV-1 carriers ($P < 0.001$) and healthy volunteers ($P < 0.001$). In contrast, those of four peaks (4067, 4151, 8130, and 8597 m/z) were significantly decreased in ATL patients ($P < 0.001$).

We focused on five peaks (1779, 1866, 2022, 4467, and 8930 m/z) whose intensities were increased in ATL, because biomarkers over-expressed in the disease state are useful target molecules for investigation, diagnosis, and chemotherapy. First, peaks of 1779, 1866, and

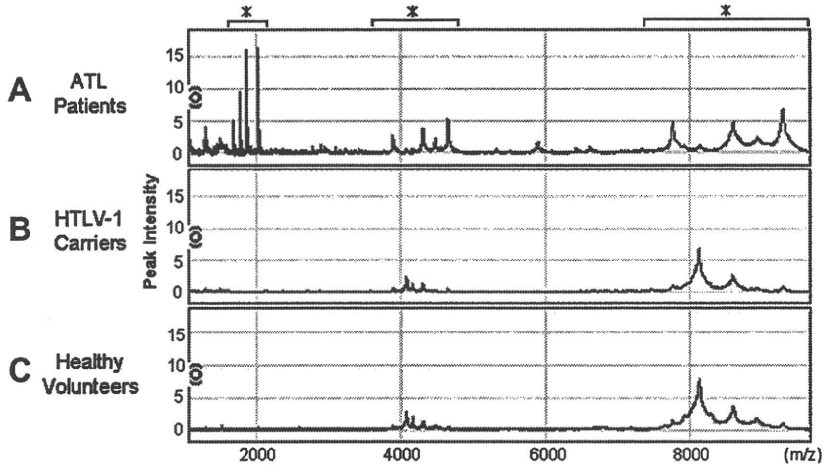

Fig. 1. Representative spectra of ATL patients, HTLV-1 carriers, and healthy volunteers. Serum samples from ATL patients, HTLV-1 carriers, and healthy volunteers were applied to CM10 ProteinChip arrays. Representative spectra of ATL patients (A), HTLV-1 carriers (B), and healthy volunteers (C) are presented. Horizontal and vertical axes indicate peptide mass to charge (m/z) and relative intensity of peaks, respectively. In the ranges of 1700–2100, 3500–5000, and 7500–10000 m/z (asterisks), the spectra of ATL patients (A) were markedly different from those of HTLV-1 carriers (B) and healthy volunteers (C).

Table 1
Peaks expressed differentially in ATL patients compared with healthy volunteers and HTLV-1 carriers on CM10 arrays[a]

m/z	ATL patients ($n = 20$)	HTLV-1 carriers ($n = 20$)		Healthy volunteers ($n = 16$)	
	Peak intensity	Peak intensity	P-value	Peak intensity	P-value
Increased					
1779	7.23 ± 6.14	0.32 ± 0.89	1.7×10^{-6}	1.13 ± 3.75	1.5×10^{-7}
1866	12.80 ± 10.66	0.56 ± 1.82	1.9×10^{-6}	1.65 ± 5.63	1.0×10^{-6}
2022	9.36 ± 8.33	1.12 ± 4.24	7.1×10^{-6}	0.67 ± 1.76	2.0×10^{-7}
4467	4.05 ± 2.39	0.52 ± 0.46	4.3×10^{-6}	0.79 ± 0.71	5.9×10^{-8}
8930	4.21 ± 2.91	0.79 ± 0.56	0.00015	1.30 ± 0.65	1.4×10^{-6}
Decreased					
4067	0.60 ± 0.46	4.03 ± 1.56	6.5×10^{-7}	3.58 ± 1.90	1.1×10^{-5}
4151	0.98 ± 0.90	2.31 ± 0.80	9.2×10^{-6}	4.44 ± 5.05	2.3×10^{-5}
8130	0.81 ± 0.49	9.22 ± 2.48	9.8×10^{-7}	7.67 ± 3.25	8.3×10^{-6}
8597	1.01 ± 0.66	1.88 ± 0.89	0.00097	2.22 ± 1.01	0.00046

[a] Data are shown as the means ± SD. Statistical differences were determined using the Mann–Whitney U test.

2022 m/z were examined in more detail (Fig. 2). As shown in Fig. 2Aa, peaks of 1779 (arrow), 1866 (arrowhead), and 2022 m/z (asterisk) were clearly detected in ATL patients. In contrast, these peaks were not detected in HTLV-1 carriers (Fig. 2Ab) and healthy volunteers (Fig. 2Ac). This was also confirmed by quantitative analysis (Fig. 2B).

Next, peaks of 4467 and 8930 m/z were examined. Considering m/z values, the peak of 4467 m/z appeared to be a doubly charged form of the 8930 m/z peak. This indicates that peptides derived from both peaks are the same; however, we failed to identify the peptide because of difficulty with its purification from serum (data not shown). Consequently, we chose peaks of 1779, 1866, and 2022 m/z as biomarker candidates of ATL.

3.2. Peptides derived from peaks of 1779, 1866, and 2022 m/z are C3f

To identify factors derived from peaks of 1779, 1866, and 2022 m/z, MS/MS ion search using tandem MS was performed [10]. MS/MS fragmentation of the peak of 2022 m/z generated a set of parent ions and fragment ions (Fig. 3). From the data set of these ions, the closest matched protein/peptide was searched by Mascot. As a result, C3f was identified. In peaks of 1866 and 1779 m/z, similar results were obtained. Table 2 shows the sequences of identified peptides. C3f of 2022 m/z was full-length C3f. C3fs of 1866 m/z and 1779 m/z had sequences deleted from full-length C3f of the 2022 m/z

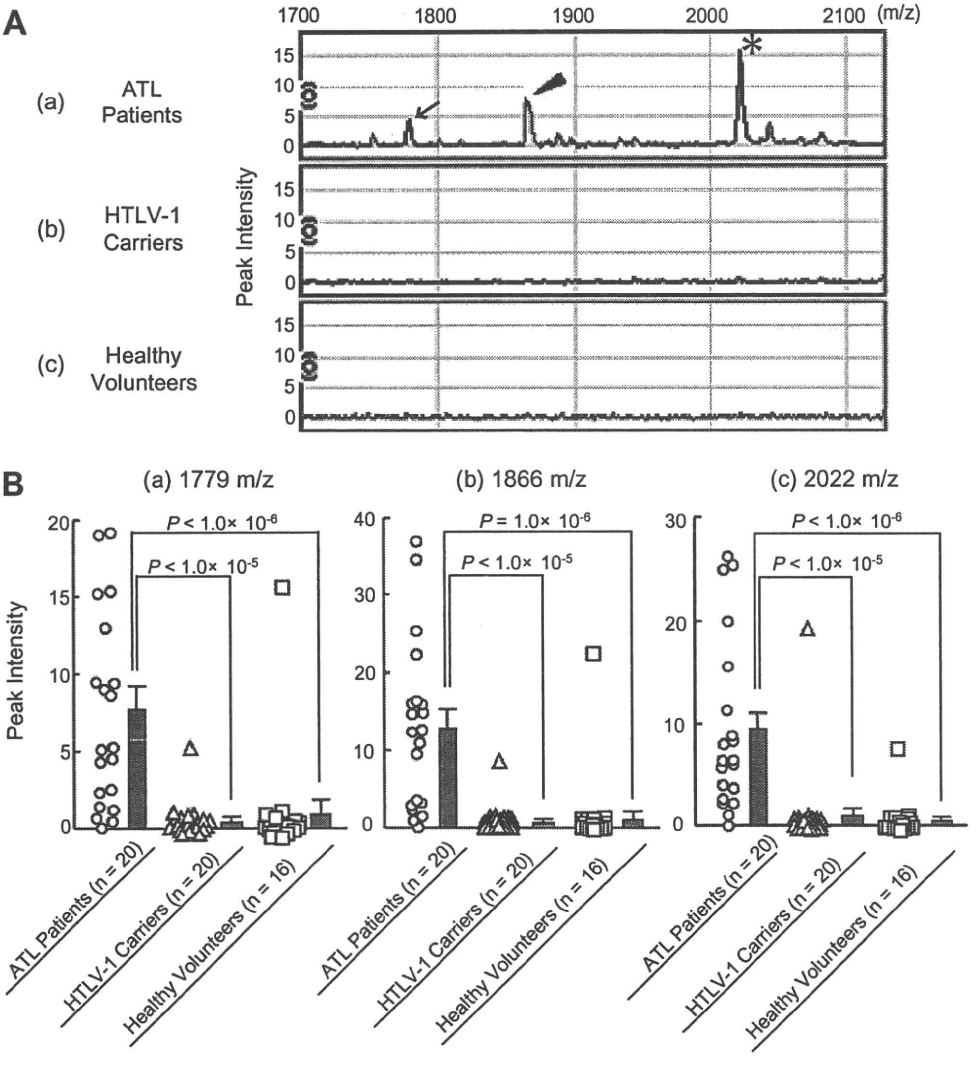

Fig. 2. Analysis of peaks of 1779, 1866, and 2022 m/z. (A) Detection of peaks of 1779, 1866, and 2022 m/z in ATL patients. In the range of 1700–2100 m/z, representative spectra were compared between ATL patients (a), HTLV-1 carriers (b), and healthy volunteers (c). Peaks of 1779 (arrow), 1866 (arrowhead), and 2022 m/z (asterisk) were detected in ATL patients (a), but not in HTLV-1 carriers (b) or healthy volunteers (c). (B) Quantitative analysis of peaks of 1779, 1866, and 2022 m/z. The intensity of peaks of 1779 (a), 1866 (b), and 2022 m/z (c) was measured by Biomarker Wizard Software. The intensity of ATL patients ($n = 20$; ○), HTLV-1 carriers ($n = 20$; △), and healthy volunteers ($n = 16$; □) was plotted. Columns represent the means ± SE. The intensity of all peaks examined was markedly increased in ATL patients (○) compared with HTLV-1 carriers (△) and healthy volunteers (□).

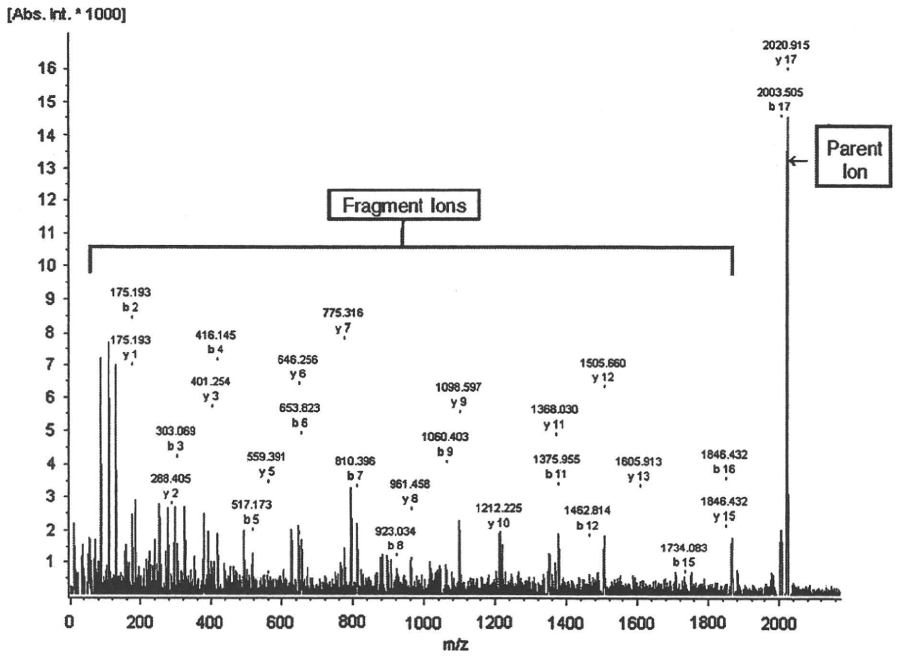

Fig. 3. MS/MS spectrum of peak of 2022 m/z. Serum sample of an ATL patient was applied to CM10 ProteinChip array, and then measured with Autoflex II TOF/TOF. Peaks of 2022 m/z (parent ion) and its fragments (fragment ions) were detected and the MS/MS spectrum was obtained.

Table 2
Identification of peptides derived from peaks of 1779, 1866, and 2022 m/z[a]

m/z	Peptide name	Accession No.	Sequence
1779	Complement C3f	gi:226159	SKITHRIHWESASLL
1866	Complement C3f	gi:226159	SSKITHRIHWESASLL
2022	Complement C3f	gi:226159	SSKITHRIHWESASLLR

[a] Identified peptides are designated with their gi Accession number of the NCBI database.

peak (Table 2). These deleted C3fs have been suggested to be generated by the action of a certain exopeptidase in serum [27].

C3f is a fragment of complement C3 [22,23]. Next, to confirm that identified peptides are derived from C3, immunoprecipitation assay was performed with anti-C3 polyclonal antibody. Serum from an ATL patient was immunoprecipitated with the antibody. As shown in Fig. 4A, in supernatants depleted of C3, the peak of 2022 m/z (asterisk in a) disappeared by treatment with anti-C3 antibody as expected (b). In immunoprecipitates, a peak of 2022 m/z was detected (asterisk in Fig. 4Bb). In contrast, peaks of 1866 and 1779 m/z did not disappear in the supernatants, which was unexpected (arrow and arrowhead in Fig. 4Ab); however, as shown in Fig. 4Bb, these peaks were detected in immunoprecipitates (arrow and arrowhead), although their intensities were weak compared with that of the peak of 2022 m/z (asterisk). C3fs of 1866 and 1779 m/z were deleted from the arginine residue of the full-length form of 2022 m/z (Table 2). Because arginine has high hydrophilicity, which is closely associated with protein antigenic determinants, the deleted C3fs may have weak affinity with anti-C3 antibody [28]. Regardless of the affinity, all peaks of 1779, 1866, and 2022 m/z were detected in immunoprecipitates, indicating that these peaks are derived from complement C3.

3.3. Activating mechanism of complement system in ATL

The complement system has three distinct pathways (classical, alternative, and lectin pathways) [23,24]. Whichever pathways are activated, C3 is finally cleaved into C3a, C3b, iC3b, and C3f etc., indicating that the increase of C3f in ATL is a reflection of the activation. Thus, the activating mechanism of the complement system in ATL was investigated.

First, to further confirm the cleavage of C3, the serum concentration of iC3b, which is generated together with C3f from C3b, was examined using enzyme immunoassay. As shown in Fig. 5, ATL patients had elevated levels of iC3b compared to HTLV-1 carriers ($P < 0.05$) and healthy volunteers ($P < 0.05$).

Next, we focused on three pathways of the complement system [23,24]. To clarify which pathways are activated in ATL, the expression of markers specific to these pathways was examined using enzyme immunoassays [29–31]. As shown in Fig. 6A, CIC concentration as a marker of the classical pathway was significantly

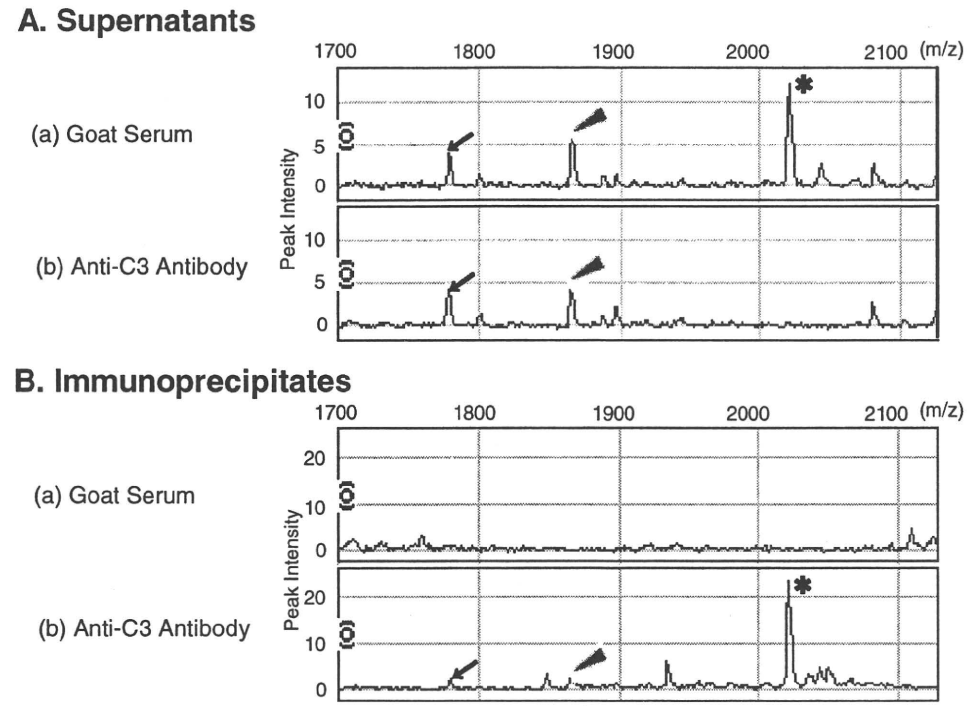

Fig. 4. Immunoprecipitation using anti-C3 antibody. Serum sample of an ATL patient was treated with goat serum (a) or anti-C3 antibody (b) followed by Protein A-Sepharose. Supernatants (A) and immunoprecipitates (B) were applied to CM10 ProteinChip arrays and then analyzed with SELDI-TOF-MS. In supernatants (A), the peak of 2022 m/z (asterisk in A-a) disappeared with anti-C3 antibody (A-b). In immunoprecipitates of the antibody (B), peaks of 1779 (arrow in B-b), 1866 (arrowhead in B-b), and 2022 m/z (asterisk in B-b) were detected.

lower in ATL patients than in HTLV-1 carriers ($P < 0.05$) and healthy volunteers ($P < 0.05$), although the pathway appears to be moderately activated in several ATL patients. A similar result was also obtained in Bb, which is a marker of the alternative pathway (Fig. 6B). Lower levels of CIC and Bb were unexpected (see Section 4). In contrast, the concentration of functional MBL/MASP-2 as a marker of the lectin pathway was significantly higher in ATL patients than in HTLV-1 carriers ($P < 0.05$) and healthy volunteers ($P < 0.05$) (Fig. 6C). Most ATL patients had higher levels of functional MBL/MASP-2. From these results, it was suggested that activation of the complement system in ATL occurred mainly through the lectin pathway.

4. Discussion

Proteomic analysis based on the separation and identification of proteins/peptides is widely used to search for biomarkers. Two-dimensional electrophoresis, liquid chromatography, and ProteinChip array are well-known tools for separation [6]. In particular, ProteinChip array has superior throughput and is successfully applied to biological fluids such as serum [6,7]. In this study, we searched for new biomarkers of ATL using ProteinChip array. The comparison of ATL patients with healthy volunteers and HTLV-1 carriers showed five increased peaks and four decreased peaks (Table 1), which have not been reported in ATL and other HTLV-1–associated diseases.

The five increased peaks and four decreased peaks are different from those reported previously by Semmes et al. [11]. The reasons for these differences may be the different sample preparations and ProteinChip array between the previous and present experiments; for example, while sera were pretreated with urea and CHAPS in the previous report, we used non-denatured serum samples. The experimental systems therefore seem responsible for the differences in detected peaks.

As a new biomarker of ATL, we identified C3f, which is a fragment of C3. Although 99% of protein content in serum is dominated by 22 proteins (e.g., albumin, immunoglobulins, lipoproteins), C3 is also one of these high abundant proteins [32]. In fact, most biomarkers identified by serum analysis using MALDI- or SELDI-TOF-MS have been reported to be highly abundant proteins and their fragments

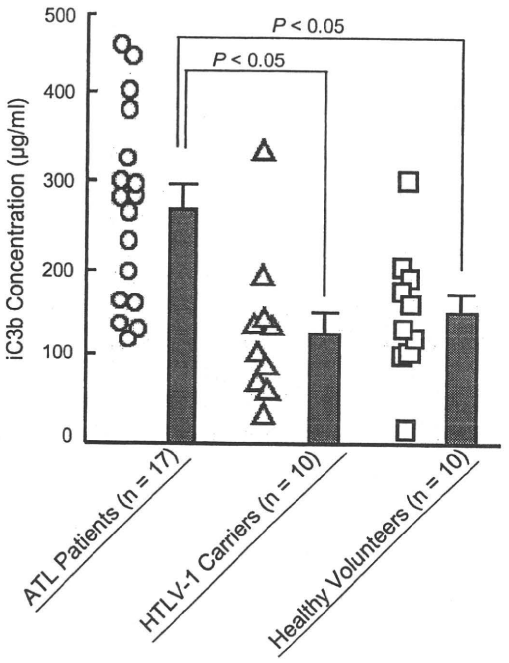

Fig. 5. Elevated levels of iC3b concentration in sera of ATL patients. The concentration of iC3b in sera of ATL patients ($n = 17$; ○), HTLV-1 carriers ($n = 10$; △), and healthy volunteers ($n = 10$; □), was examined by iC3b enzyme immunoassay kit. Columns represent the means ± SE. ATL patients (○) had elevated levels of iC3b, compared with HTLV-1 carriers (△) and healthy volunteers (□).

[33]; however, the changes in these expressions and/or processing patterns in diseases may be caused by specific molecules in pathogens. Consequently, the increase of C3f in ATL is possibly associated with a certain factor(s) specific to ATL.

The complement system is a major mediator of innate immune defense [22–24]. When pathogens exist in the living body, the system is activated, with the result that they are cleared by opsonization and/or lysis. C3 cleavage products (C3a, C3f, and iC3b) have been reported to be increased in myocardial infarction, Alzheimer's disease, nasopharyngeal cancer, breast cancer, HCC, and systemic sclerosis [27,33–38]. These findings suggest that the increase of C3f and iC3b is not specific to ATL, but common in various cancers. Also, the increase of the other C3 cleavage products (C3a and C3b etc.) is expected in ATL, because C3 is cleaved into various fragments [22–24]. In contrast to ATL, the increase was not seen in HTLV-1 carriers. These results suggest that C3 cleavage products can be used as markers for diagnosing ATL, but do not indicate a risk for ATL development in carriers. To conclude whether C3 cleavage products are useful for the diagnosis and monitoring of ATL, examining the profiles of patients with leukemia and lymphoma other than ATL might be necessary.

The mechanism by which the expression of C3 cleavage products is increased in various cancers is little understood. Our investigations of the three pathways suggested that the increase of C3f and iC3b in ATL is mainly due to activation of the lectin pathway. To further confirm this, it is necessary to examine other markers of the lectin pathway. Also, many possibilities other than pathway activation remain to be investigated. For example, the association of enzymes that cleave C3b directly might explain the mechanism. In the cleavage of C3b into C3f and iC3b, factor I serves as an enzyme of the reaction [22–24]. Besides the components of the complement system, cellular membrane type-1 matrix metalloproteinase (MT1-MMP) has been reported to cleave C3b [39]. Enzymes such as factor I and MT1-MMP may be activated in ATL and then cleave C3 directly. As another example, cross-talk between the complement and other systems is considered. The kinin system, which is involved in blood pressure regulation, is known to interact with the complement system [23]. To clarify the mechanism of the increase of C3f and iC3b in ATL, many studies are in progress.

It is of interest why the lectin pathway was activated in ATL. The lectin pathway is triggered by recognizing mannose-containing carbohydrates expressed on the surface of pathogens with MBL [23,24], and then pathogens are eventually cleared. In the course of ATL development, various abnormalities, such as the enhanced expression of genes/proteins, accumulate in HTLV-1-infected T-cells, and a fully malignant cell (ATL cell) appears [4]. Patients with ATL are profoundly immunocompromised by the impairment of cell-mediated immunity and often have opportunistic infections as ATL complications. Therefore, we can suggest two possibilities for the trigger that causes activation of the lectin pathway in ATL. The first is aberrant glycoproteins and glycolipids expressed on the surface of ATL cells. It has been reported that malignant transformation modifies the glycosylation process in cells [40–42]. The second is pathogens of opportunistic infections. It has been reported that the lectin pathway is activated against *Staphylococcus aureus* and *Candida albicans* [43–45]. Consequently, activation of the lectin pathway may be significant in the defense against ATL cells and/or opportunistic infections, although the significance remains speculative.